Squeezing in a $LiNbO_3$ integrated optical waveguide circuit

Gregory S. Kanter and Prem Kumar

Center for Photonic Communication and Computing
ECE Department, Northwestern University
Evanston, Illinois 60208-3118

kumarp@northwestern.edu

Rostislav V. Roussev, Jonathan Kurz, Krishnan R. Parameswaran, and Martin M. Fejer

E. L. Ginzton Laboratory, Stanford University
Stanford, California 94305-4085

Abstract: We report on traveling-wave quadrature squeezing generated in an integrated optical circuit fabricated with periodically-poled lithium niobate waveguides. The device integrates a second-harmonic-generation stage, waveguide couplers, spatial mode filters, and a degenerate-optical-parametric-amplification stage. The integration promises to create a low power, compact, and simple source of wideband squeezed light. −1 dB of squeezing is directly measured using 20 ps pulses with peak powers near 6W.

OCIS codes: (270.6570) Squeezed states; (190.4390) Nonlinear optics, integrated optics; (190.4410) Nonlinear optics, parametric processes; (190.4970) Parametric oscillators and amplifiers; (130.3120) Integrated optics devices; (130.3730) Lithium niobate.

References and links

1. A. Furusawa, "Amplitude squeezing of a semiconductor laser with light injection," Opt. Lett. **21**, 2014–2016 (1996).
2. K. Schneider, M. Lang, J. Mlynek, and S. Schiller, "Generation of strongly squeezed continuous-wave light at 1064 nm," Opt. Express **2**, 59–64 (1998), http://www.opticsexpress.org/abstract.cfm?URI=OPEX-2-3-59
3. Daniel Gottesman and John Preskill, "Secure quantum key distribution using squeezed states," quant-ph/0008046 **2**, 1–19 (2000).
4. C. Kim and P. Kumar, "Quadrature-squeezed light detection using a self-generated matched local oscillator", Phys. Rev. Lett. **73,** 1605-1608 (1994).
5. C. X. Yu, H. A. Haus, and E. P. Ippen, "Soliton squeezing at the gigahertz rate in a Sagnac loop," Opt. Lett. **26,** 669–671 (2001).
6. C. H. Kim, R-D Li, and P. Kumar, "Deamplification response of a traveling-wave phase-sensitive optical parametric amplifier," Opt. Lett. **19,** 132-134 (1994).
7. A. La Porta and R. E. Slusher, "Squeezing limits at high parametric gains," Phys. Rev. A **44,** 2013–2022 (1991).
8. D.K. Serkland, M.M. Fejer, R.L. Byer, and Y. Yamamoto, "Squeezing in a quasi-phase-matched $LiNbO_3$ waveguide", Opt. Lett. **20,** 1649-1651 (1995).
9. M. H. Chou, J. Hauden, M. A. Arbore, and M. M. Fejer, "1.5-μm-band wavelength conversion based on difference-frequency generation in $LiNbO_3$ waveguides with integrated coupling structures," Opt. Lett. **23** 1004-1006 (1998).
10. M. Yamada, N. Nada, M. Saitoh, and K. Wantanabe, "First-order quasi-phase matched $LiNbO_3$ waveguide periodically poled by applying an external field for efficient blue second-harmonic generation," Appl. Phys. Lett. **62,** 435–436 (1993).
11. M. L. Bortz and M. M. Fejer, "Annealed proton-exchanged $LiNbO_3$ waveguides," Opt. Lett. **16,** 1844–1846 (1991).

#761- $15.00 US
Received September 21, 2001; Revised February 04, 2002

12. D.K. Serkland, P. Kumar, M.A. Arbore, and M.M. Fejer, "Amplitude squeezing by means of quasi-phase-matched second-harmonic generation in a lithium niobate waveguide," Opt. Lett. **22,** 1497-1499 (1997).
13. M. E. Anderson, D. F. McAlister, and M. G. Raymer, "Pulsed squeezed-light generation in $\chi^{(2)}$ nonlinear waveguides," J. Opt. Soc. Am. B **14,** 3180–3190 (1997).
14. K. R. Parameswaran, M. Fujimura, R. K. Route, J. R. Kurz, R. V. Roussev, and M. M. Fejer, "Highly efficient SHG in buried waveguides formed using annealed and reverse proton exchange in PPLN," LEOS 2001, paper ThL3.

Compact and reliable sources of squeezed light are required to increase the practical applicability of squeezing. Constant-current-driven semiconductor lasers [1] and semi-monolithic optical parametric amplifiers [2] are two promising examples. However, these sources are resonant systems and, consequently, only produce squeezing inside the cavity bandwidth. Some of the most interesting applications of squeezing are in the field of quantum communications [3] and would benefit greatly from a wide-bandwidth source of squeezed light in the 1.5 μm wavelength region.

A traveling-wave degenerate optical parametric amplifier (DOPA) can produce short pulses of squeezed light with a large bandwidth [4]. The pump wave for the DOPA can be created using second-harmonic generation (SHG). The drawback is that a DOPA using bulk $\chi^{(2)}$ materials typically requires very large input powers to generate usable squeezing. Additionally, unless special precautions are taken, the noise reduction may be masked by gain-induced diffraction (GID) [6]. GID is caused by spatially-varying gain in the system owing to the use of a Gaussian-profile pump wave and forces the signal beam to diffract in an altered way. When using a typical Gaussian-profile local oscillator (LO), GID couples noisy fluctuations from the amplified quadrature into the squeezing measurement [7], degrading or eliminating the noise reduction.

A DOPA using waveguides can generate squeezing with substantially reduced input powers. For example, 14% squeezing was observed with only 0.5 W of peak second-harmonic pump power [8]. Additionally, because the signal-mode profile is determined by the waveguide geometry, GID is suppressed in such systems. An alternative to the DOPA approach is to use the Kerr ($\chi^{(3)}$) nonlinearity in optical fibers. Substantial squeezing [5] was recently reported in a soliton-based system. However, we believe $\chi^{(2)}$ based systems can offer richer control of device parameters by use of micro-fabrication techniques, such as periodic poling, and would thus lead to more functional quantum control devices.

In this work we integrate multiple functions on periodically-poled lithium niobate (PPLN) waveguides to simplify the traditional SHG/DOPA quantum-noise squeezing experiment. This is the first time, to the authors' knowledge, that highly integrated PPLN technology, which was developed for such classical applications as wavelength conversion [9], is being used in the field of quantum-noise reduction. In addition to simplifying the apparatus, the integration reduces the amount of second-harmonic lost in coupling to the DOPA stage, increasing the power efficiency of the device.

The integrated circuit is depicted in Fig. 1. A strong pump at the fundamental frequency is coupled into the center guide. A waveguide taper at the input ensures that the main waveguide region is excited in the fundamental spatial mode [9]. The fundamental frequency is converted into its second harmonic (SH) with phase matching achieved by periodic poling of the waveguide region. The residual fundamental which remains unconverted after the SH region is tapped off into the isolation guide by a properly designed wavelength dependent coupler (WDC). The generated SH travels into the DOPA region, where it is used as a pump wave for the DOPA interaction. Light can be coupled into the signal guide in order to characterize the nonlinear interactions. In our noise-reduction experiment, a vacuum field enters the signal guide and is squeezed

#761- $15.00 US Received September 21, 2001; Revised February 04, 2002

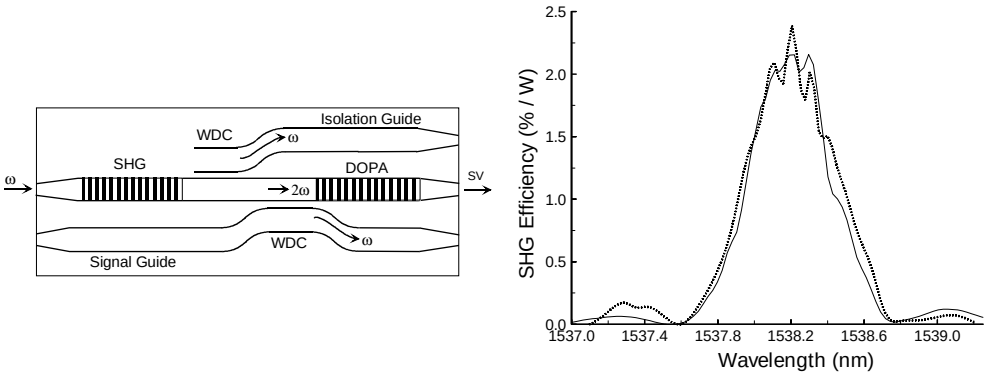

Fig. 1. Left: A schematic of the integrated squeezing circuit. Right: Phase-matching curves for the SHG (dotted curve) and DOPA (solid curve) sections. The oscillations on the curves are due to reflections from the uncoated waveguide end-faces.

by the action of the DOPA. In theory, one could also generate an amplitude-squeezed (sub-Poissonian) state by deamplifying an input coherent-state signal.

The devices are fabricated using electric-field poling [10], followed by annealed proton exchange [11]. The periodically-poled regions are 12 μm wide. Although this width leads to spatially multi-moded guides, the mode filter and adiabatic taper cause the input fundamental-frequency radiation to be coupled into its fundamental spatial mode. The SH is also generated in its fundamental spatial mode due to the phase-matching condition. These guides, therefore, behave similarly to single-moded devices, but the larger width ensures noncritical phase-matching, allowing for larger fabrication tolerances. The DOPA and SHG regions are roughly equal in length and combine to a total length of about 3.8 cm. The entire length of the sample is 5 cm. The poling period is 14.5 μm, which is designed to phase match the SHG/DOPA interactions near 1540 nm at around 90°C. The guides are not AR coated, causing 14% end-face reflections.

In order to efficiently generate squeezing, the SHG and DOPA sections need to phase match at the same wavelength. Because the two sections are located close to each other, the deviation in their phase-matching wavelength due to fabrication tolerances is small (a few tenths of a nanometer) and can be eliminated with good quality lithography. We placed the sample in a specially-constructed mount, which enabled slightly adjustable temperature differential to be maintained between the SHG and DOPA sections in order to compensate for any fabrication-related offset between the phase-matching wavelengths. A tunable CW laser was used to verify that the phase-matching tuning curves for the SHG and DOPA sections overlap [see Fig. 1(right)]. This data also shows that the temperature along the length of each section was uniform enough to yield clean tuning curves (good phase-matching).

A schematic of the squeezing experiment is shown in Fig. 2. We use a synchronously pumped (100 MHz repetition rate) color-center laser emitting $\simeq$ 20 ps pulses at 1.54 μm. The laser output is coupled into a fiber and chopped by an electro-optic modulator (EOM) to obtain low-duty-cycle (10-15%) pulse trains, which are then amplified by an erbium-doped-fiber amplifier (EDFA). The chopping allows a low-saturation-power (<10 mW) amplifier to give enough peak power to the 20 ps pulses that is adequate for the experiment. Photorefractive effects that cause inhomogeneities in the waveguide regions are reduced by elevating the operating temperature to 90°C and by maintaining low average power in the waveguides.

Due to amplified spontaneous emission (ASE) added by the EDFA, the pump for the SHG section is not shot-noise limited. It is, therefore, important to have a large

#761- $15.00 US
Received September 21, 2001; Revised February 04, 2002

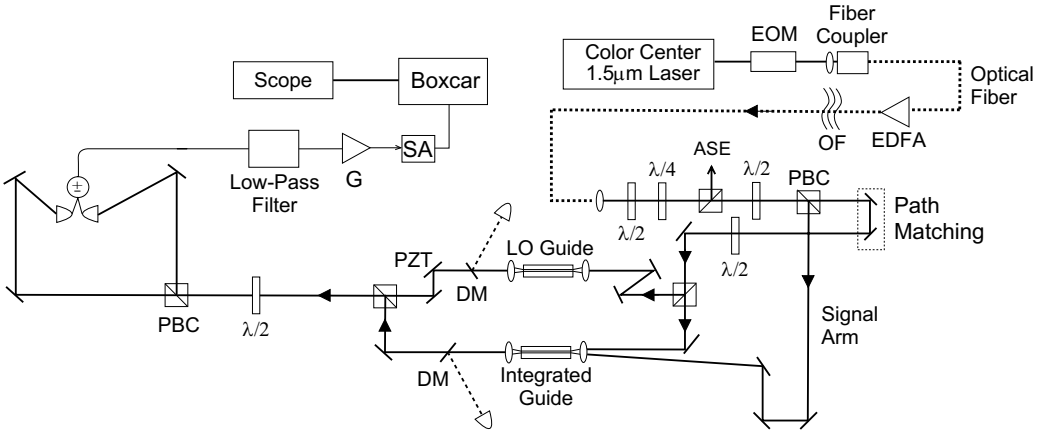

Fig. 2. A schematic of the squeezing experiment. The amplified color-center-laser beams can be made to travel to the LO guide, the center guide, or the signal guide in any ratio of powers by adjusting the waveplates ($\lambda/2$). The dichroic mirrors (DM) reflect almost all of the harmonic and a small amount of the fundamental, which are used for monitoring purposes. OF, optical filter; PZT, piezo-electric transducer.

extinction ratio between the pump deflected to the isolation guide and the residual pump (pump leakage) that transmits through the center guide [the DOPA stage from which squeezed vacuum (SV) is emitted] in order to enable proper detection of the SV output. The second WDC, which couples the input signal to the DOPA region, serves the additional purpose of further reducing the pump leakage into the DOPA stage. About 24 dB of isolation (defined as the ratio of the pump exiting the isolation guide to that exiting the center guide) is provided by the two WDCs. Also, because the pump leakage exiting the center guide is that small quantity of the fundamental-frequency pump which is not properly filtered by the two WDCs, it is not predominantly in the fundamental spatial mode of the waveguide. This is ensured by measuring the mode-matching efficiency (MME) (via interference fringes) between the fundamental light coupled into the signal guide and the pump leaking out from the center guide. The MME is found to be less than 10%. This implies that during squeezing measurement via balanced homodyne detection the main effect of the pump leakage is simply to increase the shot-noise level (SNL) by an amount directly proportional to the leakage power. The mode overlap between the LO and the pump leakage is poor and any excess noise on the pump is subtracted out by the balanced detectors.

Some of the fundamental-frequency light amplified by the EDFA is tapped off for use as a LO. The tapped-off beam is passed through a separate waveguide that was fabricated in the same way as the integrated guide. This enables us to obtain good spatial MME ($86 \pm 5\%$) between the beam exiting the separate guide (the LO) and and signal mode of the integrated guide (the SV).

The LO and DOPA outputs are combined 50/50 on a polarization beam cube (PBC) and sent to resonant detectors [12] for noise measurement via balanced homodyne detection (see Fig. 2). The 50/50 power split is created by proper adjustment of a half-wave plate ($\lambda/2$) placed before the PBC. The common-mode-rejection ratio of the balanced detectors is over 35 dB. The photocurrent difference from the detectors is filtered by a 50-MHz low-pass filter and amplified by a 40dB-gain low-noise amplifier (G) before being sent to a spectrum analyzer (SA). Noise measurements are performed at 42 MHz (the resonant frequency of the detectors) with a 3 MHz resolution bandwidth. The 3-MHz-wide video output from the spectrum analyzer is fed into a boxcar averager in order to sample the readings at the peak of the chopping window. Such synchronous de-

#761- $15.00 US Received September 21, 2001; Revised February 04, 2002

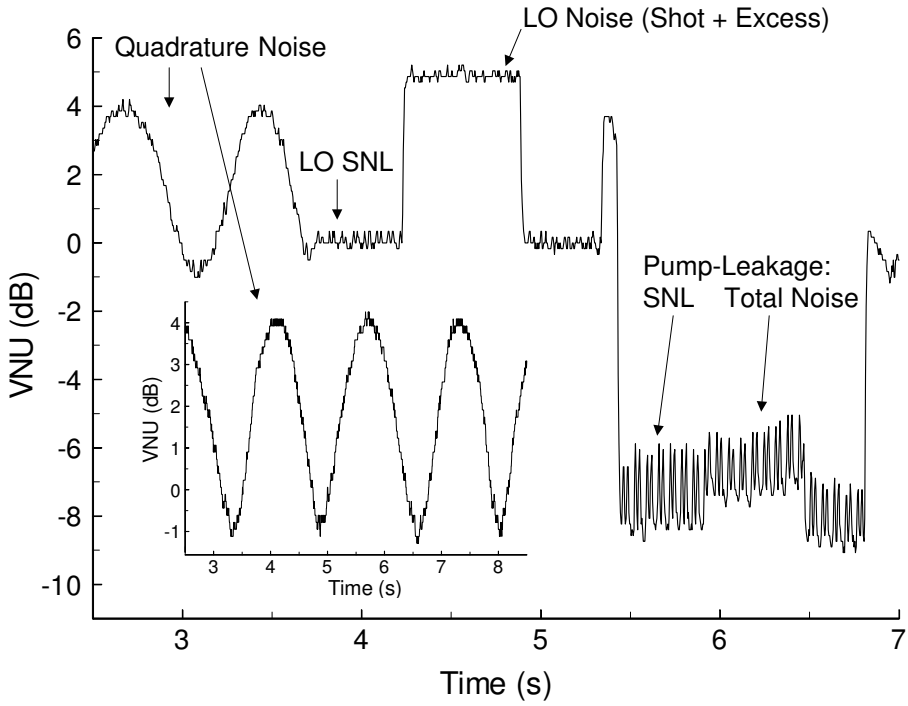

Fig. 3. Noise measurements of several types are shown here including (from left to right) the quadrature-noise measurements as a PZT varies the phase between the LO and the SV, the LO SNL, the LO total-noise level (about 5 dB of excess noise), and the pump-leakage shot- and excess-noise levels.

tection enables the shot noise of our low-average-power (<80 μW) LO to be well above the electronic noise floor of the instrumentation.

The photocurrents from the two detectors are subtracted during homodyne measurement of the SV. The SNL is calibrated by blocking the output from the center guide. The excess noise on the LO can be measured by summing the photocurrents. The actual LO SNL is slightly lower than the SNL observed during the SV measurement; the latter getting contribution from the mode-mismatched pump leakage. Therefore, in order to directly see the noise reduction by comparison with the LO SNL, the pump leakage must be much smaller than the LO. However, if the fundamental pump power is decreased to reduce the pump leakage, the generated squeezing is also decreased. Therefore, the splitting ratio between the LO and the pump is chosen to maximize the directly observed squeezing, balancing these two effects.

Figure 3 shows the squeezed and anti-squeezed quadrature noise measurement, along with the LO SNL, the excess noise on the LO, the pump-leakage SNL, and the excess noise on the pump leakage during a measurement. These readings are taken by either adding or subtracting the photocurrents of the two homodyne detectors while the various beams are being blocked. The noise of the detection electronics has been subtracted from these data. The figure inset focuses on the quadrature noise measurement. As shown, about -1 dB of squeezing and 4 dB of anti-squeezing are directly observed. We can estimate our detection efficiency by multiplying the various factors that contribute to it: the detectors' quantum efficiency (0.85), the spatial MME (0.86), the reduced transmittance due to Fresnel back reflection at the waveguide end-face (0.84), and the reduced transmittance caused by the various linear optical losses from the waveguide end-face to the photodiodes (0.95). This leads to a 58% total detection efficiency, which is

#761- $15.00 US
Received September 21, 2001; Revised February 04, 2002

an overestimate because losses in the DOPA waveguide and reduced temporal MME are not accounted for. The latter is due to the SV being temporally modified by the nonlinear effects (which are intensity dependent) and the group-velocity mismatch between the SH and fundamental wavelengths in the DOPA guide (about 3.7 ps/cm). The negative effect on squeezing of such temporal mode-matching problems will be described in more detail in another work.

The data in Fig. 3 allows us to estimate the importance of the shot noise due to the pump leakage. However, because this noise level is less than 2 dB above the instrumentation noise floor, its measurement is quite inaccurate. Therefore, we conservatively estimate that the LO noise is at most 8 dB above the pump-leakage noise, suggesting that the correct SNL during the SV measurement is actually 0.6 dB higher than that depicted in Fig. 3. Thus, if this leakage is eliminated, the magnitude of the squeezing measured would increase to $\simeq$ 1.6 dB (the anti-squeezing would correspondingly be reduced by 0.6 dB). While one can account for the pump leakage with an independent noise (or power) measurement, the presence of this leakage is undesirable, and we are developing a mode-selective loss element to be integrated in the device to further reduce the leakage magnitude.

The average input pump power incident on the nonlinear waveguide is about 1.6 mW. This corresponds to about 6 W of peak power for the 20 ps pulses, which is further reduced upon entering the waveguide due to the end-face reflection and coupling inefficiency. 270 μW of SH power (about 1 W peak power) exits the DOPA guide. This represents orders of magnitude less power than that required in the -1.4 dB squeezing result of Anderson *et al.* [13], which is the largest amount of squeezing yet observed in traveling-wave $\chi^{(2)}$ waveguides.

In conclusion, we have demonstrated an integrated optical circuit for generating wideband squeezed light in a compact and simple manner. The integration of a SHG stage and a DOPA stage with the required WDCs also serves to increase the overall power efficiency of the device, since it eliminates the difficult task of properly coupling the SH from a SHG waveguide to a separate DOPA waveguide. We obtained -1 dB of directly-measured squeezing at very low pump powers, which would improve to -1.6 dB with elimination of the pump leakage, as discussed above, and to -2 dB with AR coating of the end-face. Furthermore, recent improvements in waveguide fabrication techniques have yielded devices that are three times more efficient than the one used in this paper. [14] We anticipate that such efficiency increase in an integrated squeezing device would lead to improved signal deamplification ($\simeq$ 0.32 in the present device), yielding up to -3 dB of squeezing for the same input fundamental pump power and overall detection efficiency. And by implementing matched LO techniques to further increase the detection efficiency, [6] it is possible to obtain directly-observable squeezing values better than -4 dB from such integrated devices. We believe that with further refinements, integrated waveguide devices can become important in the field of quantum communications.

This work was supported in part by grants from the National Science Foundation (ECS-9821109 and ECS-9903156).

#761- $15.00 US Received September 21, 2001; Revised February 04, 2002